Article **Journal of Experimental Systems**
December, 2021 Vol.8 No.25 13-21

Robust linearization scheme by structural state feedback for a quadrotor

Esquema de linealización robusta por realimentación de estado estructural para un cuadricóptero

BLAS-SÁNCHEZ, Luis Ángel†*, GALINDO-MENTLE, Margarita, QUIROZ-RODRÍGUEZ, Adolfo and LICONA-GONZÁLEZ, Marlon

Universidad Tecnológica de Xicotepec de Juárez, Ingeniería en Mantenimiento Industrial, Av. Universidad Tecnológica No. 1000, Col. Tierra Negra, C.P. 73080, Cd. Xicotepec de Juárez, Pue., México

ID 1st Author: *Luis Ángel, Blas-Sánchez* / **ORC ID**: 0000-0003-3313-8551, **Researcher ID Thomson**: AAX-2475-2021, **arXiv Author ID**: AnghelBlas and **CVU CONACYT ID**: 554052

ID 1st Coauthor: *Margarita, Galindo-Mentle* / **ORC ID**: 0000-0001-5390-5960, **Researcher ID Thomson**: S-9202-2018, **arXiv Author ID**: MargaritaG, **CVU CONACYT-ID**: 160164

ID 2nd Coauthor: *Adolfo, Quiroz-Rodríguez* / **ORC ID**: 0000-0002-9685-9455, **Researcher ID Thomson**: S-9189-2018, **arXiv Author ID**: adolfo-79, **CVU CONACYT ID**: 105471

ID 3rd Coauthor: *Marlon, Licona-González* / **ORC ID**: 0000-0001-7829-4457, **Researcher ID Thomson**: AAR-6259-2021, arXiv Author ID marlon1987, **CVU CONACYT-ID**: 1138370

DOI: 10.35429/JOES.2021.25.8.13.21 Received: July 30, 2021; Accepted November 30, 2021

Abstract

In this work a feedback linearization technique is proposed, to carry it out to linearize the dynamic model of the quadrotor, a change of variable is introduced that maps the nonlinearities of the system into a nonlinear uncertainty signal contained in the domain of the action of control and is applied to the dynamic model of the quadrotor. To estimate the nonlinear uncertainty signal, the Beard-Jones filter is used, which is based on standard state observers. To verify the effectiveness of the proposed control scheme, experiments are carried out outdoors to follow a circular trajectory in the (x, y) plane. This presented control scheme is suitable for unmanned aerial vehicles where it is important to reject not only non-linearities but also to seek the simplicity and effectiveness of the control scheme for its implementation.

Linearization, Trajectory tracking, Quadrotor aircraft

Resumen

En este trabajo se presenta una técnica de linealización por realimentación para linealizar el modelo dinámico del cuadricóptero, para llevarla a cabo, se introduce un cambio de variable que mapea las no linealidades del sistema en una señal de incertidumbre no lineal contenida en el dominio de la acción de control y se aplica al modelo dinámico del cuadricóptero. Para estimar la señal de incertidumbre no lineal se utiliza el filtro Beard-Jones, el cual se basa en observadores de estado estándar. Para verificar la efectividad del esquema de control propuesto, se realizan experimentos en exteriores para el seguimiento de una trayectoria circular en el plano (x, y). Este esquema de control presentado es adecuado para vehículos aéreos no tripulados donde es importante rechazar no solo las no linealidades sino también buscar la simplicidad y efectividad del esquema de control para su implementación

Linealización, Seguimiento de trayectoria, Cuadricóptero

Citation: BLAS-SÁNCHEZ, Luis Ángel, GALINDO-MENTLE, Margarita, QUIROZ-RODRÍGUEZ, Adolfo and LICONA-GONZÁLEZ, Marlon. Robust linearization scheme by structural state feedback for a quadrotor. Journal of Experimental Systems. 2021. 8-25: 13-21

* Author Correspondence (luisangel.blas@utxicotepec.edu.mx)
† Researcher contributing as first author.

Introduction

One type of rotary-wing aerial vehicle that has received considerable attention in recent years is quadrotor. These small unmanned helicopters have the capability of vertical takeoff and landing and hovering. Due to their compact size, high maneuverability, and autonomous flight, they have become a standard platform for aerial robotics research around the world.

Unmanned aerial vehicles can be used in many applications such as: earth science, search and rescue, border surveillance, industrial inspection, agriculture, research, etc. This is due to its ease of deployment, low maintenance cost, and hover capability. Unmanned aerial vehicles have been introduced academically as the subject of research projects. The basic dynamic model of the quadrotor is the starting point for all studies carried out. More complete dynamic models have also been obtained by including engine dynamics and aerodynamic effects (Dong et al, 2013), (Hoffmann et al, 2007).

Recently, there has been a great interest in finding simple and effective control schemes for unmanned aerial vehicles (UAVs), capable of rejecting non-linearities and unexpected structure changes. These control schemes must be simple and effective, since they must be programmed in the autopilot incorporated into the quadcopter.

In the literature you can consult the different control techniques that have been evaluated, among them are the Proportional-Derivative (PD) controller (Michael et al, 2010), (Can Dikmen et al, 2009), Proportional-Integral-Derivatice (PID) controller (Bouabdallah et al, 2004), (Li et al, 2011), backstepping controller (Madani et al, 2006), (Huo et al, 2014), non-linear H-infinity controller (V. Raffo et al, 2010), LQR controller (Bouabdallah et al, 2004), sliding modes control and non-linear controllers with nested saturations (Castillo et al, 2005), (Escareno et al, 2006).

A natural and simple control scheme for these non-linear systems is to use the classical Taylor approximation. This is indeed a very simple approach. However, the corresponding techniques must be restricted to a small neighborhood of a fixed reference point.

Under some restrictive assumptions related to external disturbance, this technique can be useful for kinds of regulation problems. On the other hand, it is not recommended, for example, in tracking control problems. Another simple control scheme is the exact input-output linearization technique. This analytical approach requires a complete knowledge of the parameters of the dynamic model, as well as the corresponding derivatives.

Orientation and trajectory tracking control designs based on an inner/outer loop control structure have been presented for normal flight conditions (Li et al, 2010). A robust controller based on the time scale separation approach has been proposed to achieve automatic take-off, hovering, trajectory tracking, and landing missions for a quadcopter (Liu et al, 2014). A state feedback solution is presented to the problem of stabilizing a quadcopter along a predefined trajectory in the presence of constant force disturbances. These disturbances are estimated through the use of adaptive backstepping (Cabecinhas et al, 2014).

A double closed-loop disturbance active rejection control scheme is presented to address some difficult control problems in the quadcopter such as non-linearity, strong coupling, and disturbance sensitivity (Zhang et al, 2018).

This work presents the development and implementation of a control scheme capable of rejecting the non-linearities of the system and compensating for unexpected changes in structure.

Methodology

Dynamic model

To obtain the dynamic model, we consider the quadrotor as a rigid object in three-dimensional space, subjected to a main force and three moments. A rigid body in three-dimensional space has the following generalized coordinates

$$q = \begin{bmatrix} \xi \\ \eta \end{bmatrix} \in \mathbb{R}^6 \quad (1)$$

ISSN 2410-3950

where $\xi = [x \quad y \quad z]^T \in \mathbb{R}^3$ denotes the position vector of the center of mass of the quadrotor relative to the inertial reference frame I. $\eta = [\phi \quad \theta \quad \psi]^T \in \mathbb{R}^3$ expresses the Euler angles with respect to the inertial reference frame, ϕ is the roll angle around the x axis, θ is the pitch angle around the y axis and ψ is the yaw angle around the z axis (García *et al* 2012), (V. Cook, 2013). The positive directions of these angles are chosen according to the right hand rule.

The equations that describe the translational and rotational dynamics are:

$$m\begin{bmatrix} d^2x/dt^2 \\ d^2y/dt^2 \\ d^2z/dt^2 \end{bmatrix} = \begin{bmatrix} u_z(c_\phi s_\theta c_\psi + s_\phi s_\psi) \\ u_z(c_\phi s_\theta s_\psi - s_\phi c_\psi) \\ u_z(c_\phi c_\theta) + mg \end{bmatrix} \quad (2)$$

$$J\ddot{\eta} = \tau - C(\eta, \dot{\eta})\dot{\eta} \quad (3)$$

where m is the mass of the quadcopter, u_z is the main control input or main force applied to the vehicle which is generated by the four rotors, $\tau = [\tau_\phi \quad \tau_\theta \quad \tau_\psi]^T \in \mathbb{R}^3$ represents the roll, pitch and yaw moments, J acts as the inertia matrix for the total rotational kinetic energy of the quadrotor, $C(\eta, \dot{\eta})$ is known as the Coriolis term and contains gyroscopic and centrifugal effects associated with η.

Incremental model

In order to compensate for gravity, the following control law is proposed:

$$u_z = \Delta u_z - mg \quad (4)$$

The expressions of the translational and rotational dynamics are obtained:

$$\begin{bmatrix} d^2x/dt^2 \\ d^2y/dt^2 \\ d^2z/dt^2 \end{bmatrix} = \begin{bmatrix} -\theta g \\ \phi g \\ \frac{1}{m}\Delta u_z \end{bmatrix} + \begin{bmatrix} q_x \\ q_y \\ q_z \end{bmatrix} \quad (5)$$

$$\begin{bmatrix} d^2\phi/dt^2 \\ d^2\theta/dt^2 \\ d^2\psi/dt^2 \end{bmatrix} = \begin{bmatrix} u_y/I_{xx} \\ u_x/I_{yy} \\ u_\psi/I_{zz} \end{bmatrix} + \begin{bmatrix} q_\phi \\ q_\theta \\ q_\psi \end{bmatrix} \quad (6)$$

Where

$$\begin{aligned} q_x &= \theta g - q_{xx} g + \tfrac{1}{m}\Delta u_z q_{xx} \\ q_y &= -\phi g - q_{yy} g + \tfrac{1}{m}\Delta u_z q_{yy} \\ q_z &= -q_{zz} g + \tfrac{1}{m}\Delta u_z q_{zz} \end{aligned} \quad (7)$$

And

$$\begin{aligned} q_{xx} &= c_\phi s_\theta c_\psi + s_\phi s_\psi \\ q_{yy} &= c_\phi s_\theta s_\psi - s_\phi c_\psi \\ q_{zz} &= c_\phi c_\theta \end{aligned} \quad (8)$$

$$\begin{bmatrix} q_\phi \\ q_\theta \\ q_\psi \end{bmatrix} = \left(J^{-1}(\eta) - J^{-1}(0)\right)\tau - J^{-1}(\eta)\, C(\eta, \dot{\eta})\dot{\eta} \quad (9)$$

where q_x, q_y and q_z describe the non-linear part of the translational dynamics, q_ϕ, q_θ and q_ψ describe the non-linear part of the rotational dynamics and $u_y = \tau_\phi$, $u_x = \tau_\theta$ and $u_\psi = \tau_\psi$ are control actions.

State space representations

From equations (5) and (6) the state representations ($i \in \{x, y, z, \psi\}$) are obtained:

$$\frac{d}{dt}\mathrm{x}_i = \mathbf{A}_i \mathrm{x}_i + \mathbf{B}_i u_i + \mathbf{S}_i \mathbf{q}_{oi}, \quad y_i = \mathbf{C}_i \mathrm{x}_i, \quad (10)$$

$$\mathbf{A}_x = \begin{bmatrix} 0 & 1 & 0 & 0 \\ 0 & 0 & -g & 0 \\ 0 & 0 & 0 & 1 \\ 0 & 0 & 0 & 0 \end{bmatrix}, \mathbf{A}_y = \begin{bmatrix} 0 & 1 & 0 & 0 \\ 0 & 0 & g & 0 \\ 0 & 0 & 0 & 1 \\ 0 & 0 & 0 & 0 \end{bmatrix},$$
$$\mathbf{B}_x = I_{yy}^{-1}\boldsymbol{B}_4, \mathbf{B}_y = I_{xx}^{-1}\boldsymbol{B}_4, \mathbf{S}_x = \mathbf{S}_y, \mathbf{C}_x = \mathbf{C}_y,$$
$$\mathbf{B}_4 = \begin{bmatrix} 0 \\ 0 \\ 0 \\ 1 \end{bmatrix}, \mathbf{S}_y = \begin{bmatrix} 0 & 0 \\ 1 & 0 \\ 0 & 0 \\ 0 & 1 \end{bmatrix}, \mathbf{C}_y = \begin{bmatrix} 0 \\ 0 \\ 0 \\ 1 \end{bmatrix}^T \quad (11)$$

$$\mathbf{A}_z = \mathbf{A}_\psi = \begin{bmatrix} 0 & 1 \\ 0 & 0 \end{bmatrix}, \quad \mathbf{B}_z = M_q^{-1}B_2, \quad \mathbf{B}_\psi = I_{zz}^{-1}B_2, \mathbf{S}_z = \mathbf{S}_\psi = \boldsymbol{B}_2, \mathbf{B}_2 = \begin{bmatrix} 0 \\ 1 \end{bmatrix}, \ \mathbf{C}_z = \mathbf{C}_\psi = \begin{bmatrix} 1 \\ 0 \end{bmatrix}^T \quad (12)$$

where $\mathrm{x}_x = \begin{bmatrix} x & dx/dt & \theta & d\theta/dt \end{bmatrix}^T$, $\mathrm{x}_y = \begin{bmatrix} y & dy/dt & \phi & d\phi/dt \end{bmatrix}^T$, $\mathrm{x}_z = \begin{bmatrix} z & dz/dt \end{bmatrix}^T$, $\mathrm{x}_\psi = \begin{bmatrix} \psi & d\psi/dt \end{bmatrix}^T$, $\mathbf{q}_{ox} = \begin{bmatrix} q_x & q_\theta \end{bmatrix}^T$, $\mathbf{q}_{oy} = \begin{bmatrix} q_y & q_\phi \end{bmatrix}^T$, $\boldsymbol{q}_{oz} = q_z$, $\boldsymbol{q}_{o\psi} = q_\psi$. The nonlinear signals q_x, q_y, q_z, q_ϕ, q_θ q_ψ were defined in (7) and (9).

Locally stabilizing feedback

To locally stabilize (10)-(12), the state feedback gain vectors were obtained using the LQR design, that is, the optimal feedback gain matrix is obtained by solving the Riccati algebraic equation:

$$\mathbf{A}_i^T\mathbf{P}_i + \mathbf{P}_i\mathbf{A}_i - \mathbf{P}_i\mathbf{B}_i(\rho_i I)^{-1}\mathbf{B}_i^T\mathbf{P}_i + \mathbf{Q}_i = 0 \quad (13)$$

ISSN 2410-3950

where $i \in \{x, y, z, \psi\}$ and:

$$\mathbf{Q}_x = \mathbf{Q}_y = 900\begin{bmatrix}1 & 0 & 0 & 0\\ 0 & 0 & 0 & 0\\ 0 & 0 & 1 & 0\\ 0 & 0 & 0 & 2.25\end{bmatrix},\ \mathbf{Q}_z = \begin{bmatrix}1 & 0\\ 0 & 0.23\end{bmatrix},\ \mathbf{Q}_\psi = \begin{bmatrix}1 & 0\\ 0 & 0.6\end{bmatrix} \quad (14)$$

$$\rho_x = \rho_y = 1,\ \rho_z = \frac{1}{12100},\ \rho_\psi = \frac{1}{19600} \quad (15)$$

Solving (13) with (11), (12), (14) and (15) for $i \in \{\mathrm{x}, \mathrm{y}, \mathrm{z}, \psi\}$ we obtain for the following state feedbacks:

$$\mathbf{u}_i = \mathbf{F}_i \mathrm{x}_i + \bar{\mathbf{u}}_i,\ i \in \{x, y\} \quad (16)$$

and

$$\mathbf{u}_i = \mathbf{F}_i(\mathrm{x}_i - \bar{\mathrm{x}}_i),\ \ i \in \{z, \psi\}, \quad (17)$$

the optimal state feedback gain vectors:

$$\mathbf{F}_x = \begin{bmatrix}30 & 32.43 & -171.92 & -45.05\end{bmatrix},\ \mathbf{F}_y = \begin{bmatrix}-30 & -32.43 & -171.92 & -45.05\end{bmatrix},\ \mathbf{F}_z = [-140 \quad -69.92],\ \mathbf{F}_\psi = [-110 \quad -85.24] \quad (18)$$

Linearization by structural state feedback

Let's consider the following variable change:

$$\zeta_i = x_i + \mathbf{M}_i \mathbf{C}_{(\mathbf{M}_i, \mathbf{S}_i)} \boldsymbol{\Psi}_n(d^j/dt^j)\, q_{oi}(x, \mathrm{u}) \quad (19)$$

where $\mathbf{C}_{(\mathbf{M}_i, \mathbf{S}_i)} = [S \quad MS \quad \cdots \quad M^{n-1}S]$ and $\boldsymbol{\Psi}_n\left(\frac{d^j}{dt^j}\right) = [\mathrm{I} \quad \mathrm{I}d/dt \quad \cdots \quad \mathrm{I}d^{n-1}/dt^{n-1}]^T$.

State representations (10) feedback with (16) and (18) are written as ($i \in \{x, y\}$):

$$\frac{d}{dt}\zeta_i = \mathbf{A}_{F_i}\zeta_i + \mathbf{B}_i\left(\bar{\boldsymbol{u}}_i + \mathbf{q}_{*i}(\mathbf{x}_i, \mathbf{u}_i)\right),\ \ y_i = \mathbf{C}_i\zeta_i \quad (20)$$

Thus, the exact linearization by structural state feedback is $\bar{\boldsymbol{u}}_i = \mathbf{q}_{*i}(\mathbf{x}_i, \mathbf{u}_i)$, where $\mathbf{A}_{F_i} = \mathbf{A}_i + \mathbf{B}_i\mathbf{F}_i$ and the nonlinear uncertainty signal $\mathbf{q}_{*i}$ is:

$$\mathbf{q}_{*i}(\mathbf{x}_i, \mathbf{u}_i) = \mathbf{X}_i \mathbf{C}_{(\mathbf{M}_i, \mathbf{S}_i)} \boldsymbol{\Psi}_n(d^j/dt^j)\, q_{oi}(\mathbf{x}, \mathbf{u}) \quad (21)$$

where the matrices $\mathbf{M}_i$ and $\mathbf{X}_i$ are solutions of the equation:

$$\mathbf{A}_{F_i}\mathbf{M}_i + \mathbf{B}_i\mathbf{X}_i = \mathrm{I} \quad (22)$$

Nonlinear uncertainty signal estimator

To estimate the nonlinear uncertainty signals, an estimator based on the Beard-Jones filter (V. Beard. 1971), (Bonilla, M. *et al*, 2016) is synthesized for (11):

$$\frac{d}{dt}\mathbf{w}_i = \left(\mathbf{A}_{\mathbf{K}_i} + \mathbf{B}_i\mathbf{G}_i^\ell\mathbf{C}_i\right)\mathbf{w}_i - \left(\mathbf{K}_i + \mathbf{B}_i\mathbf{G}_i^\ell\right)\mathbf{y}_i,$$
$$\bar{\mathbf{u}}_i = \mathbf{G}_i^\ell(\boldsymbol{C}_i\mathbf{w}_i - \mathbf{y}_i) \quad (23)$$

where $\mathbf{A}_{\mathbf{K}_i} = \mathbf{A}_{F_i} + \mathbf{K}_i\mathbf{C}_i$ and $\boldsymbol{G}_i^\ell = -(\boldsymbol{C}_i\boldsymbol{A}_{\mathrm{K}_i}^{-1}\boldsymbol{B}_i)^\ell$ for $i \in \{x, y\}$.

$$\mathbf{A}_{F_i} = \begin{bmatrix}0 & 0 & 0 & -a_{i,4}\\ 1 & 0 & 0 & -a_{i,3}\\ 0 & 1 & 0 & -a_{i,2}\\ 0 & 0 & 1 & -a_{i,1}\end{bmatrix},\ \mathbf{B}_i = \begin{bmatrix}0\\ 0\\ 0\\ -g/I_{yy}\end{bmatrix}, \mathbf{C}_i = \begin{bmatrix}0\\0\\0\\1\end{bmatrix}, \mathbf{K}_i = \begin{bmatrix}a_{i,4} - a_{i_{o,4}}\\ a_{i,3} - a_{i_{o,3}}\\ a_{i,2} - a_{i_{o,2}}\\ a_{i,1} - a_{i_{o,1}}\end{bmatrix}, \quad (24)$$

where $a_{i,1}$, $a_{i,2}$, $a_{i,3}$ and $a_{i,4}$ are the coefficients of the Hurwitz polynomial $\pi_{x_i}(s) = \det(\mathrm{sI} - \mathbf{A}_{F_i}) = s^4 + a_{i,1}s^3 + a_{i,2}s^2 + a_{i,3}s + a_{i,4}$.

The transfer function of the closed-loop system is:

$$\mathrm{F}_{CL}(s) = \mathrm{F}_{\zeta_x}(s)(1 - \mathrm{F}_{e_x}(s)) \quad (25)$$

where

$$\mathrm{F}_{\zeta_i}(s) = \mathbf{C}_i(\mathrm{sI} - \mathbf{A}_{F_i})^{-1}\mathbf{B}_i = \frac{g}{I_{yy}\,\pi_{x_i}(s)} \quad (26)$$

$$1 - \mathrm{F}_{e_x}(s) = 1 - \boldsymbol{G}_i^\ell\mathbf{C}_i\left(\mathrm{sI} - \mathbf{A}_{\mathbf{K}_i}\right)^{-1}\mathbf{B}_i = 1 - \frac{a_{i_{o,4}}}{\pi_{e_i}(s)} = \frac{s\bar{\pi}_{\omega_i}(s)}{\pi_{e_i}(s)} \quad (27)$$

where $\pi_{x_i}(s)$, $\pi_{e_i}(s)$ and $\bar{\pi}_{\omega_i}(s)$ are Hurwitz polynomials.

$$\pi_{e_i}(s) = \det(\mathrm{sI} - \mathbf{A}_{\mathbf{K}_i}) = s^4 + a_{i_{o,1}}s^3 + a_{i_{o,2}}s^2 + a_{i_{o,3}}s + a_{i_{o,4}} \quad (28)$$

$$\bar{\pi}_{\omega_i}(s) = s^3 + a_{i_{o,1}}s^2 + a_{i_{o,2}}s + a_{i_{o,3}} \quad (29)$$

And the polynomials $\pi_{e_i}(s)$ and $\bar{\pi}_{\omega_i}(s)$ are related as follows:

$$\pi_{e_i}(s) = s\bar{\pi}_{\omega_i}(s) + a_{i_{o,4}} \quad (30)$$

Using the root locus procedure, we obtain:

$$\pi_{e_i}(s) = (s+1)(s^2 + 10.25s + 28.125) \quad (31)$$

Scaling the polynomial (31) for $i \in \{x, y\}$ by a positive constant ϱ_{e_x} we obtain:

$$\pi_{e_i}(s) = \left(s + \varrho_{e_x}\right)\left(s^2 + 10.25\varrho_{e_x}s + 28.125{\varrho_{e_x}}^2\right) \quad (32)$$

With $\varrho_{e_x} = 18$ experimentally a good performance was obtained and the polynomial (32) is:

$$\pi_{e_i}(s) = s^4 + 220.5s^3 + 16078.5s^2 + 387828s + 2952450 \quad (33)$$

Drift-free estimator

Experimentally, the nonlinear uncertainty signal estimator (23) performs well when the quadcopter is hovering. However, when we want the quadcopter to follow some trajectory in the (x, y), plane, sometimes the quadcopter exhibits a drift phenomenon.

To overcome the drift we have proceeded as in (P. Gavin, P. *et al*, 1998) and (Horowitz *et al*, 1989), shifting the pole of the origin of (23) slightly to the left of the complex plane. That is, the root of the characteristic polynomial:

$$\pi_{\omega_i}(s) = \det\left(s\mathbf{I}_4 - \left(\mathbf{A}_{\mathbf{K}_i} + \mathbf{B}_i\mathbf{G}_i^{\ell}\mathbf{C}_i\right)\right) = s\bar{\pi}_{\omega_i}(s) = s\left(s^3 + a_{i_{o,1}}s^2 + a_{i_{o,2}}s + a_{i_{o,3}}\right) \quad (34)$$

it is shifted to the left. For this, the parameter $\epsilon a_{i_{o,4}}$ is added, where ϵ is a sufficiently small positive constant. This modification of the characteristic polynomial (34) is achieved by slightly reducing the gain $\boldsymbol{G}_i^{\ell}$ of the nonlinear uncertainty signal estimator (23), that is:

$$\frac{d}{dt}\mathbf{w}_{df,i} = \left(\mathbf{A}_{\mathbf{K}_i} + (1-\epsilon)\mathbf{B}_i\mathbf{G}_i^{\ell}\mathbf{C}_i\right)\mathbf{w}_{df,i} - \left(\mathbf{K}_i + (1-\epsilon)\mathbf{B}_i\mathbf{G}_i^{\ell}\right)\mathbf{y}_i, \quad \bar{\mathbf{u}}_{df,i} = (1-\epsilon)\mathbf{G}_i^{\ell}(\boldsymbol{C}_i\mathbf{w}_{df,i} - \mathbf{y}_i) \quad (35)$$

where $i \in \{x, y\}$.

Notice that the characteristic polynomial of $\mathbf{A}_{\mathbf{K}_i} + (1-\epsilon)\mathbf{B}_i\mathbf{G}_i^{\ell}\mathbf{C}_i$ has no roots at the origin:

$$\pi_{\omega_{df,i}}(s) = \det\left(s\mathbf{I} - \left(\mathbf{A}_{\mathbf{K}_i} + (1-\epsilon)\mathbf{B}_i\mathbf{G}_i^{\ell}\mathbf{C}_i\right)\right)$$
$$\pi_{\omega_{df,i}}(0) = \det\left(\mathbf{A}_{\mathbf{K}_i}\right)\det\left(-1 - (1-\epsilon)\,\mathbf{C}_i\mathbf{A}_{\mathbf{K}_i}^{-1}\mathbf{B}_i\mathbf{G}_i^{\ell}\right) = -\epsilon \neq 0 \quad (36)$$

From (35) and (20), the closed-loop system is:

$$\frac{d}{dt}\begin{bmatrix} e_{df,i} \\ \zeta_i \end{bmatrix} = \mathbf{A}_{CL_{df,i}}\begin{bmatrix} e_{df,i} \\ \zeta_i \end{bmatrix} + \mathbf{B}_{CL_i}\mathbf{q}_{*i},$$
$$\mathbf{y}_i = \mathbf{C}_{CL_i}\begin{bmatrix} e_{df,i} \\ \zeta_i \end{bmatrix} \quad (37)$$

$$\mathbf{A}_{CL_{df,i}} = \begin{bmatrix} \mathbf{A}_{\mathbf{K}_i} & 0 \\ (1-\epsilon)\mathbf{B}_i\mathbf{G}_i^{\ell}\mathbf{C}_i & \mathbf{A}_{\mathbf{F}_i} \end{bmatrix}, \mathbf{B}_{CL_i} = \begin{bmatrix} -\mathbf{B}_i \\ \mathbf{B}_i \end{bmatrix}, \mathbf{C}_{CL_i} = [0 \quad \mathbf{C}_i] \quad (38)$$

where $e_{df,i} = \mathbf{w}_{df,i} - \zeta_i$.

The transfer function of $\Sigma(\mathbf{A}_{CL_{df,i}}, \mathbf{B}_{CL_i}, \mathbf{C}_{CL_i})$ is:

$$\mathrm{F}_{CL_{df,i}}(s) = \mathbf{C}_{CL_i}\left(\mathrm{sI} - \mathbf{A}_{CL_{df,i}}\right)^{-1}\mathbf{B}_{CL_i} = \mathrm{F}_{\zeta_i}(s)(1 - \mathrm{F}_{e_{df,i}}(s)) \quad (39)$$

where:

$$\mathrm{F}_{e_{df,i}}(s) = (1-\epsilon)\mathbf{G}_i^{\ell}\mathbf{C}_i\left(\mathrm{sI} - \mathbf{A}_{\mathbf{K}_i}\right)^{-1}\mathbf{B}_i \quad (40)$$

From (35) and (40) we obtain the polynomials:

$$\pi_{\omega_{df,i}}(s) = \det\left(s\mathbf{I} - \left(\left(\mathbf{A}_{\mathbf{K}_i} + \mathbf{K}_i\mathbf{C}_i\right) + (1-\epsilon)\,\mathbf{B}_i\mathbf{G}_i^{\ell}\mathbf{C}_i\right)\right) = s\bar{\pi}_{\omega_i}(s) + \epsilon a_{i_{o,4}} \quad (41)$$

$$\mathrm{F}_{e_{df,i}}(s) = (1-\epsilon)a_{i_{o,4}}/\pi_{e_i}(s) \quad (42)$$

Trajectory tracking

For the experiments carried out outdoors when the quadrotor follows a circular trajectory of 5 m radius in the (x, y) plane, proceed as follows: the quadcopter is stabilized locally with the LQR and robustly linearized with the drift-free estimators (35), an optimal state trajectory is synthesized to go from a local stationary point to the next local stationary point of the circular trajectory and finally the circular trajectory is partitioned by a finite set of local stationary points.

The local stabilizing feedbacks (16) and the drift-free estimators (35) are written as:

$$\mathbf{u}_i = \mathbf{F}_i(\mathrm{x}_i - \mathrm{x}_i^*) + \bar{\mathbf{u}}_{df,i} \quad (43)$$

$$\frac{d}{dt}\mathbf{w}_{df,i} = \left(\mathbf{A}_{\mathbf{K}_i} + (1-\epsilon)\mathbf{B}_i\mathbf{G}_i^{\ell}\mathbf{C}_i\right)\mathbf{w}_{df,i} - \left(\mathbf{K}_i + (1-\epsilon)\mathbf{B}_i\mathbf{G}_i^{\ell}\right)\boldsymbol{C}_i(\mathrm{x}_i - \mathrm{x}_i^*),\ \bar{\mathbf{u}}_{df,i} = (1-\epsilon)\mathbf{G}_i^{\ell}(\boldsymbol{C}_i\mathbf{w}_{df,i} - \boldsymbol{C}_i(\mathrm{x}_i - \mathrm{x}_i^*)) \quad (44)$$

where $i \in \{x, y\}$ and together with (18) and (24). We want to solve the following control problem, let the linear systems described by the state representations (*cf.* (10), (11), (16) and (18)), consider the linear description in state space:

$$\frac{d}{dt}\mathrm{x}_i^* = \mathbf{A}_{\mathbf{F}_i}\mathrm{x}_i^* + \mathbf{B}_i\bar{\mathbf{u}}_i^*, \qquad i \in \{x, y\} \quad (45)$$

where $\mathbf{A}_{\mathbf{F}_i} = \mathbf{A}_i + \mathbf{B}_i\mathbf{F}_i,\ i \in \{x, y\}$, such that the pairs $(\mathbf{A}_{\mathbf{F}_i}, \mathbf{B}_i)$ are controllable (*cf.* (11)).

Let $\mathrm{x}_i^*(t)$ be a partition of the desired trajectory for $i \in \{x, y\},\ t \in [0, T_f]$ at $N+1$ stationary points, that is:

$$\Lambda_{SP_i}^* = \{\bar{\mathrm{x}}_{0,i}^*, \bar{\mathrm{x}}_{1,i}^*, \bar{\mathrm{x}}_{2,i}^*, \ldots, \bar{\mathrm{x}}_{N,i}^*\},\ \mathrm{x}_i^*(kT_s) = \bar{\mathrm{x}}_{k,i}^* \quad (46)$$

where $k \in \{0, 1, 2, \ldots, N\}$, $NT_s = T_f$ and $i \in \{x, y\}$; T_s is the trajectory sampling time and T_f is the flight time.

We are interested in finding minimum norm control inputs $\bar{\mathbf{u}}_i^*$ such that the solution trajectories, starting from the stationary point $\mathrm{x}_i^*(kT_s) = \mathrm{x}_{k,i}$, reach the next stationary point in finite time, that is: $\mathrm{x}_i^*((k+1)T_s) = \bar{\mathrm{x}}_{(k+1),i}^*$ where T_s is the given sampling time, $T_s > 0$.

This classical minimum norm problem consists of finding the vector closest to the origin that lies in a finite codimension manifold, in a Hilbert space, and is solved with the help of the projection theorem.

According to Theorem 2 of Section 3.3 of (G. Luenberger, 1969), the control input $\bar{\mathbf{u}}_i^*$ to solve the problem has the form:

$$\bar{\mathbf{u}}_i^*(t) = -\mathcal{F}_{F_i}(T_s - t)\mathfrak{W}_{i_{T_s}}^{-1}\exp\left(\boldsymbol{A}_{\boldsymbol{F}_i}T_s\right)\mathrm{x}_{o,i},\ i \in \{\mathrm{x}, \mathrm{y}\}, t \in [0, T_f] \quad (47)$$

Where

$$\mathcal{F}_{F_i} = \mathbf{B}_i^T\exp\left(\mathbf{A}_{\mathbf{F}_i}^T t\right),$$

$$\mathfrak{W}_{i_{T_s}} = \int_0^{T_s}\mathcal{F}_{\boldsymbol{F}_i}^T(T_s - \tau)\mathcal{F}_{\boldsymbol{F}_i}(T_s - \tau)d\tau \quad (48)$$

From (45), (47) and (48) we obtain for all time intervals $[kT_s, (k+1)T_s)$, $k \in \{0, 1, 2, \ldots, (N-1)\}$, the following optimal trajectories:

$$\mathrm{x}_i^*(t) = \exp\left(\boldsymbol{A}_{\boldsymbol{F}_i}(t - kT_s)\right)\bar{\mathrm{x}}_{k,i}^* + \int_{kT_s}^{t}\mathcal{F}_{\mathbf{F}_i}^T(t - \tau)\beta_i^*(t, \tau)v_{k,i}^*d\tau \quad (49)$$

Where

$$\beta_i^*(t, \tau) = \mathcal{F}_{\mathbf{F}_i}(t - \tau)\mathfrak{W}_{i_{T_s}}^{-1},$$
$$v_{k,i}^* = \mathrm{x}_{(k+1),i}^* - \exp\left(\mathbf{A}_{\mathbf{F}_i}T_s\right)\bar{\mathrm{x}}_{k,i}^*,$$
$$\bar{\mathrm{x}}_{k,i}^* = \Lambda_{SP_i}^*, i \in \{\mathrm{x}, \mathrm{y}\} \quad (50)$$

We are interested in following a circular trajectory:

$$\mathrm{x}_*^2(t) + (\mathrm{y}_*(t) - \boldsymbol{r}_*)^2 = \boldsymbol{r}_*^2 \quad (51)$$

this is:

$$\mathrm{x}_*(t) = \boldsymbol{r}_*\sin(\omega_s t)$$
$$\mathrm{y}_*(t) = \boldsymbol{r}_*(1 - \cos(\omega_s t)) \quad (52)$$

where $\omega_s = 2\pi/T_s$. Partitioning T_f in N points we obtain $(t = (k/N)T_s, k \in \{0, 1, 2, \ldots, (N-1)\}$.

$$\left(\bar{x}_{k,x}^*, \bar{x}_{k,y}^*\right) = r_*([\sin(\alpha_k) \quad \omega_s\cos(\alpha_k) \quad \left(\frac{\omega_s^2}{g}\right)\mathrm{sen}(\alpha_k) \quad \left(\frac{\omega_s^3}{g}\right)\cos(\alpha_k)]^T,\ [\left(1 - \cos(\alpha_k)\right) \quad \omega_s\sin(\alpha_k) \quad \left(\frac{\omega_s^2}{g}\right)\cos(\alpha_k) \quad \left(\frac{\omega_s^3}{g}\right)\sin(\alpha_k)]^T) \quad (53)$$

where $\alpha_k = 2\pi k/N$.

Results

Experimental platform

The quadcopter used in the experiments is built on a carbon fiber structure with a length of 498 mm. The Pixhawk flight controller has the following features: a 32-bit STM32F427 Cortex-M4F microprocessor with FPU, 168 MHz, 256 KB of RAM and 2 MB Flash. It has the I2C, PWM interfaces, 5x UART serial ports, two ADC inputs, Spektrum DSM and Futaba inputs.

ISSN 2410-3950

It has the following sensors integrated: magnetometer, barometer, two accelerometers and two gyroscopes. Use an external Ublox Neo-M8N GPS with compass. To power the electronics and motors, LiPo batteries with a capacity of 4000 mAh, three cells and a discharge rate of 45C are used. The quadrotor's propulsion system is composed of four 16-pole 4220-880Kv motors and four 11x4.5-inch propellers.

Figure 1 Quadrotor

Experimental results

The experimental results performed outdoors are presented to follow a circular trajectory tracking of radius $\boldsymbol{r}_* = 5$ m in the (x, y) plane. We consider the following steps: the quadrotor is stabilized locally with the state feedbacks (43) for $i \in \{\mathrm{x}, \mathrm{y}, \psi\}$ and for $i = \mathrm{z}$ we use (17) and (18). The quadcopter is robustly linearized with the drift-free estimators (44) for $i \in \{x, y, \psi\}$ together with (24), (33) and $\epsilon = 1/50$. The circular trajectory for tracking is generated with the help of (48), (49), (50) and (53) with $\boldsymbol{r}_* = 5$ m and $T_s = 1$ s.

A circular trajectory (51) was followed with radius $\boldsymbol{r}_* = 5$ m, sampling time $T_s = 1$s and a partition of $N = 20$ points, that is: $T_s = 20$ s. Graphics 2 to 4 show the results obtained when the locally stabilizing feedbacks (43) are applied with and without the drift free estimators (44). In Graphic 1 the trajectory obtained is compared with the desired circular trajectory. In Graphic 2 the trajectories (x, y) obtained are compared with the reference trajectories. The tracking error $e_c(t)$ is shown in Graphic 3:

$$e_c(t) = \sqrt{(x(t) - x_*(t))^2 + (y(t) - \mathrm{y}_*(t))^2} \quad (54)$$

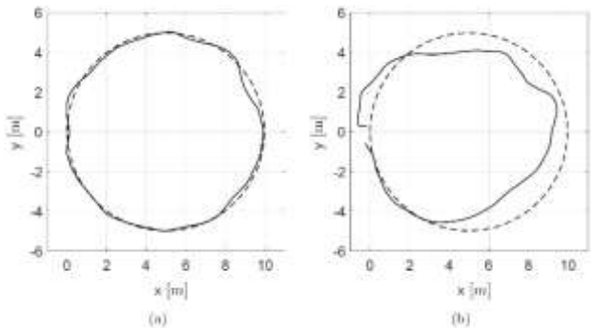

Graphic 1 Circular trajectory tracking in the (x, y) plane with a radius of 5 m in $20\,s$ ($N = 20$ y $T_s = 1$ s). (a) Application of locally stabilizing feedbacks together with drift free estimators. (b) Applying only locally stabilizing feedbacks.

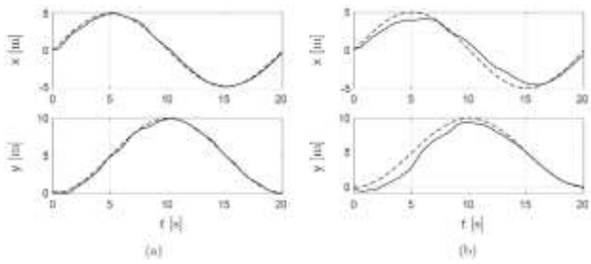

Graphic 2 Comparison of the trajectories in (x, y) with the references. (a) Application of locally stabilizing feedbacks together with drift free estimators. (b) Applying only locally stabilizing feedbacks.

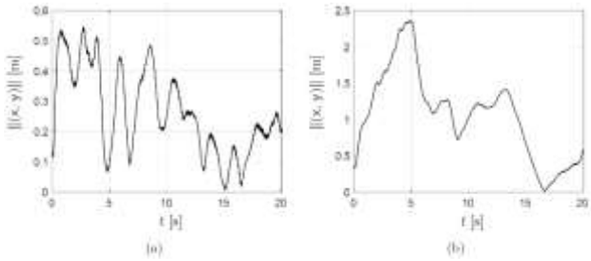

Graphic 3 Comparison of tracking error $e_c(t)$. (a) Application of locally stabilizing feedbacks together with drift free estimators. (b) Applying only locally stabilizing feedbacks.

When the locally stabilizing feedbacks (43) are applied together with the drift free estimators (44), we obtain the maximum error peak $\|e_c\|_p = 0.5463$ m and the mean square error $\|e_c\|_{rms} = 0.2992$ m where:

$$\|e_c\|_p = \max_{t \in [0, T_f]} e_c(t),$$

$$e_c(t) = \sqrt{\frac{1}{T_f} \int_0^{T_f} e_c^2(t) dt} \quad (55)$$

ISSN 2410-3950

When only locally stabilizing feedbacks are applied (43) we obtain the maximum error peak $\|e_c\|_p = 0.9493$ m and the mean square error $\|e_c\|_{rms} = 0.5534$ m.

Conclusions

In this article it was shown that a non-linear system modeled by the state representation (10) can be transformed to the state representation (20). In (10) the non-linearities characterized by the non-linear disturbance signal vector q_{oi}, which acts through S_i. In (20) the nonlinearities are characterized by the non-linear uncertainty signal vector q_{*i}, acting directly through B_i. This transformation is achieved by the change of variable (19), which exists under conditions of torque controllability (A_i, B_i). Since now the nonlinear uncertainty signal q_{*i} (21) acts through B_i, then it can be canceled directly by the control input $\bar{u}_i$.

The exact linearization is based on the analytical reconstruction of q_{*i}; but if this is not possible, it can be estimated. For this, the nonlinear uncertainty signal estimator (23) was proposed based on the Beard-Jones filter, whose objective is to robustly reject the nonlinear uncertainty signal q_{*i}.

Trajectory tracking was addressed and it was found that there is a drift phenomenon when we want the quadcopter to follow some trajectory in the (x, y) plane, to overcome this quadcopter drift phenomenon, it was proposed to shift slightly to the left of the plane complex to the pole at the origin of (23), obtaining the drift free estimator (35).

To circular trajectory tracking in the (x, y) plane, an optimal state trajectory was synthesized (49) and the circular trajectory was partitioned into a finite set of local stationary points (53).

In the outdoor experimental results when the quadcopter follows a circular trajectory of radius 5 m in the (x, y) plane, an appreciable reduction in tracking errors was obtained when applying the drift-free estimators.

References

Dong, W., Gu, G. Y., Zhu, X., & Ding, H. (2013, May). Modeling and control of a quadrotor UAV with aerodynamic concepts. In Proceedings of World Academy of Science, Engineering and Technology (No. 77, p. 437). World Academy of Science, Engineering and Technology (WASET).

Hoffmann, G., Huang, H., Waslander, S., & Tomlin, C. (2007, August). Quadrotor helicopter flight dynamics and control: Theory and experiment. In AIAA guidance, navigation and control conference and exhibit (p. 6461).

Michael, N., Mellinger, D., Lindsey, Q., & Kumar, V. (2010). The grasp multiple micro-uav testbed. IEEE Robotics & Automation Magazine, 17(3), 56-65.

Dikmen, İ. C., Arisoy, A., & Temeltas, H. (2009, June). Attitude control of a quadrotor. In 2009 4th International Conference on Recent Advances in Space Technologies (pp. 722-727). IEEE.

Bouabdallah, S., Noth, A., & Siegwart, R. (2004, September). PID vs LQ control techniques applied to an indoor micro quadrotor. In 2004 IEEE/RSJ International Conference on Intelligent Robots and Systems (IROS)(IEEE Cat. No. 04CH37566) (Vol. 3, pp. 2451-2456). IEEE.

Li, J., & Li, Y. (2011, August). Dynamic analysis and PID control for a quadrotor. In 2011 IEEE International Conference on Mechatronics and Automation (pp. 573-578). IEEE.

Madani, T., & Benallegue, A. (2006, October). Backstepping control for a quadrotor helicopter. In 2006 IEEE/RSJ International Conference on Intelligent Robots and Systems (pp. 3255-3260). IEEE.

Huo, X., Huo, M., & Karimi, H. R. (2014). Attitude stabilization control of a quadrotor UAV by using backstepping approach. Mathematical Problems in Engineering, 2014.

Raffo, G. V., Ortega, M. G., & Rubio, F. R. (2010). An integral predictive/nonlinear H∞ control structure for a quadrotor helicopter. Automatica, 46(1), 29-39.

ISSN 2410-3950

Castillo, P., Lozano, R., & Dzul, A. (2004, September). Stabilization of a mini-rotorcraft having four rotors. In 2004 IEEE/RSJ International Conference on Intelligent Robots and Systems (IROS)(IEEE Cat. No. 04CH37566) (Vol. 3, pp. 2693-2698). IEEE.

Escareno, J., Salazar-Cruz, S., & Lozano, R. (2006, June). Embedded control of a four-rotor UAV. In 2006 American Control Conference (pp. 6-pp). IEEE.

Zhou, Q. L., Zhang, Y., Rabbath, C. A., & Theilliol, D. (2010, October). Design of feedback linearization control and reconfigurable control allocation with application to a quadrotor UAV. In 2010 Conference on Control and Fault-Tolerant Systems (SysTol) (pp. 371-376). IEEE.

Liu, H., Bai, Y., Lu, G., Shi, Z., & Zhong, Y. (2014). Robust tracking control of a quadrotor helicopter. Journal of Intelligent & Robotic Systems, 75(3), 595-608.

Cabecinhas, D., Cunha, R., & Silvestre, C. (2014). A nonlinear quadrotor trajectory tracking controller with disturbance rejection. Control Engineering Practice, 26, 1-10.

Zhang, Y., Chen, Z., Zhang, X., Sun, Q., & Sun, M. (2018). A novel control scheme for quadrotor UAV based upon active disturbance rejection control. Aerospace science and technology, 79, 601-609.

Carrillo, L. R. G., López, A. E. D., Lozano, R., & Pégard, C. (2012). Quad rotorcraft control: vision-based hovering and navigation. Springer Science & Business Media.

Cook, M. V. (2012). Flight dynamics principles: a linear systems approach to aircraft stability and control. Butterworth-Heinemann.

Beard, R. V. (1971). Failure accomodation in linear systems through self-reorganization (Doctoral dissertation, Massachusetts Institute of Technology).

Bonilla, M., Blas, L. A., Salazar, S., Martínez, J. C., & Malabre, M. (2016, June). A robust linear control methodology based on fictitious failure rejection. In 2016 European Control Conference (ECC) (pp. 2596-2601). IEEE.

Gavin, H. P., Morales, R., & Reilly, K. (1998). Drift-free integrators. Review of scientific instruments, 69(5), 2171-2175.

Horowitz, P., Hill, W., & Robinson, I. (1989). The art of electronics (Vol. 2, p. 658). Cambridge: Cambridge university press.

Luenberger, D. G. (1997). Optimization by vector space methods. John Wiley & Sons.

ISSN 2410-3950